

# Texel-Att: Representing and Classifying Element-based Textures by Attributes

Marco Godi\*<sup>1</sup>

marco.godi@univr.it

Christian Joppi\*<sup>1</sup>

christian.joppi@univr.it

Andrea Giachetti<sup>1</sup>

andrea.giachetti@univr.it

Fabio Pellacini<sup>2</sup>

pellacini@di.uniroma1.it

Marco Cristani<sup>1</sup>

marco.cristani@univr.it

<sup>1</sup> Department of Computer Science

University of Verona

Strada le Grazie 15, Italy

<sup>2</sup> Sapienza, University of Rome

Rome,

Italy

\* These authors contributed equally to this work.

## Abstract

Element-based textures are a kind of texture formed by nameable elements, the *texels* [1], distributed according to specific statistical distributions; it is of primary importance in many sectors, namely textile, fashion and interior design industry. State-of-the-art texture descriptors fail to properly characterize element-based texture, so we present *Texel-Att* to fill this gap. *Texel-Att* is the first fine-grained, attribute-based representation and classification framework for element-based textures. It first individuates texels, characterizing them with individual attributes; subsequently, texels are grouped and characterized through layout attributes, which give the *Texel-Att* representation. Texels are detected by a Mask-RCNN, trained on a brand-new element-based texture dataset, *ElBa*, containing 30K texture images with 3M fully-annotated texels. Examples of individual and layout attributes are exhibited to give a glimpse on the level of achievable graininess. In the experiments, we present detection results to show that texels can be precisely individuated, even on textures “in the wild”; to this sake, we individuate the element-based classes of the Describable Texture Dataset (DTD), where almost 900K texels have been manually annotated, leading to the *Element-based DTD* (E-DTD). Subsequently, classification and ranking results demonstrate the expressivity of *Texel-Att* on *ElBa* and E-DTD, overcoming the alternative features and relative attributes, doubling the best performance in some cases; finally, we report interactive search results on *ElBa* and E-DTD: with *Texel-Att* on the E-DTD dataset we are able to individuate within 10 iterations the desired texture in the 90% of cases, against the 71% obtained with a combination of the finest existing attributes so far. Dataset and code is available at <https://github.com/godimarcovr/Texel-Att>

## 1 Introduction

*Element-based* textures [1, 2, 3, 4] are textures formed by nameable recognizable elements, also dubbed *texels* [1], organized according to specific spatial distributions (see



Figure 1: (a) Examples of element-based textures in the DTD [5]: the *dotted* (left) and *banded* (right) classes are examples where texels are dots and bands, respectively; (b) Zalando shows for each clothing a particular one on the texture; (c) examples of DTD [5] textures which are *not* element-based: (*marbled* on top and *porous* on bottom); here is hard to find clearly nameable local entities; (d) examples of *EIBA* textures: polygon on top, multi-class lined+circle texture on bottom.

Fig. 1a-b). They differ from those textures whose main characteristics are defined merely at a *micro* scale, *i.e.*, focusing on materials and material properties (see Fig. 1c).

Element-based textures are of particular importance in the textile, fashion and interior design industry, with thousands of products (clothes, floor tiles, furniture) stored in vast catalogues or websites that the user (shopper, or designer) has to explore to find the preferred item to buy or to take inspiration from [13, 14]; Fig. 1b illustrates two examples taken from the popular e-commerce Zalando where, as many other fashion companies are doing now, clothing items are always accompanied by zoomed pictures highlighting textures. In these scenarios, describing textures and their compositional structure with communicative and intuitive features is of primary importance, in order to give a precise semantic content-based blueprint that allows a fast retrieval [23] or to design usable interfaces for professionals or casual users that create and print their own textile as in the web applications of *Patternizer*, *Contrado*, *Spoonflower*, *DesignYourFabric*, to quote some.<sup>1</sup>

Attribute-based texture features [4, 5, 15, 20] are explicitly suited to give textures nameable yet discriminative descriptions, and have been shown to excel in texture classification tasks. The most-known texture attributes are the 47 perceptually-driven ones like *dotted*, *woven*, *lined*, etc., that can be learned on the Describable Texture Dataset (DTD) [5]. It is worth noting a limitation of these attributes: they describe the properties of a texture image *as it was a whole atomic entity*: for example, in Fig. 1a, two different (element-based) attributes are considered, and specifically: *dotted* (left) and *banded* (right). For each attribute, two representative images are arranged in a column. Despite the same attribute that characterizes them, the images are strongly different: on the left, the top image has more, smaller dots; on the right, the top image has thin bands, while on the bottom bands are thick. In the Zalando examples (Fig. 1b), both the clothes come with the same attribute (“checked”), despite their diversity (squares have strongly different dimensions).

In all cases, it is evident that for a finer expressivity one needs to focus on the recognizable *texels* that constitute the textures.

In this paper, we present *Texel-Att*, a fine-grained, attribute-based texture representation and classification framework for element-based textures.

<sup>1</sup><https://patternizer.com/d0Wp>, <https://www.contrado.com/>, <https://www.spoonflower.com/> and <https://designyourfabric.ca/> respectively.

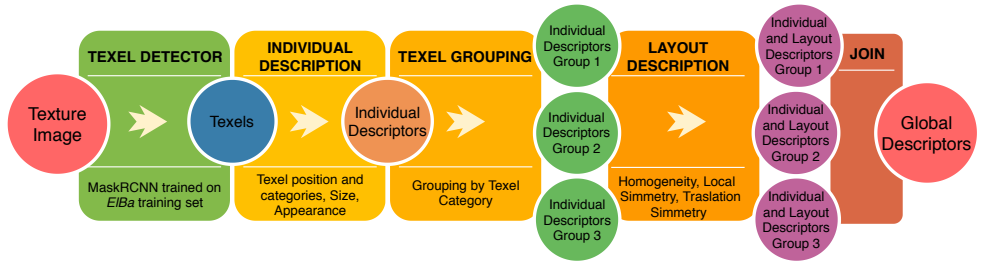


Figure 2: Block diagram of the formation of the Texel-Att element-based texture descriptor. On the bottom of each plate, the specific choices made in this paper, which can be varied.

The representation pipeline of Texel-Att detects first the single texels, assigning them *individual attributes*. Subsequently, texels are grouped depending on the individual attributes, and groups of texels receive *layout attributes*.

Individual and layout attributes form the Texel-Att final description of the texture, that can be used for classification and retrieval. It is worth noting that the Texel-Att descriptor has no pre-defined dimensionality, as it depends on the attributes one does use. In this paper, we just give some examples to illustrate the general framework.

The texel detection is performed by a Mask-RCNN [10], showing that element-based descriptions can be individuated with current state-of-the-art detection architectures (despite the fact that further improvements are foreseeable as we will discuss later). To train (and test) the detector, we design the first *Element-Based* texture dataset, *ElBa*, taking inspiration by the many online catalogues and printing services cited above. *ElBa* is composed of procedurally-generated realistic renderings, where we vary in a *continuous* way element shapes and colors and their distribution, to generate 30K texture images with different local symmetry, stationarity, and density of (3M) localized texels, whose attributes are thus known by construction.

In the experiments, we show that texels can be detected with high precision on *ElBa*, and even on textures in the wild. To this sake, we consider the DTD [5], selecting the 12 element-based classes and manually labeling the related almost 900K texels, originating the Element-based DTD (E-DTD). Subsequently, we show texture classification results where the pitfalls of current texture descriptors [4, 25] do emerge, failing to classify toy examples where instead Texel-Att succeeds.

Beyond the mere classification, Texel-Att descriptions induce reliable partial ordering so beating relative attributes [24] learned with alternative descriptors on ranking experiments. This fact is exploited in the final experiment to accelerate interactive image search [14], where a user is asked to find his desired texture among large repositories. Texel-Att allows to reach the goal with a lower number of steps, paving the way for commercial applications.

## 2 The Texel-Att Framework

Fig. 2 shows a block diagram of the Texel-Att description creation pipeline. Briefly speaking, a customized region proposal method processes input images, extracting texels that subsequently are assigned with *individual* attributes, *i.e.*, labelled according to specific texel categories, and characterized with properties related to appearance and size. Individually la-

beled texels are then grouped, filtered (discarding non-repeated texels) and *layout* attributes describing the spatial layout of groups are estimated. Individual and layout attributes form the composite Texel-Att descriptor. In the following, each processing block is detailed.

**Texel Detector.** The texel detection is built on the Mask-RCNN [10] model, which localizes and classifies objects providing bounding boxes and segmentation masks. We learn the model on the training partition of the *ElBa* dataset, allowing to detect and classify as *lines*, *circles*, *polygons* potentially each texel in a given image (see Sec. 3). The message here is that the texels, whose detection a few years ago was quite complicated and limited to specific scenarios (*i.e.*, lattices [9, 13]), are now easily addressable in whatsoever displacement.

**Individual description of texels.** Each detected texel is characterized with attributes related to shape properties and human perception, and in particular: (i) the *label* provided by the Mask-RCNN, indicating its shape; (ii) main *color* given by a color naming procedure [27] (with 11 possible colors); (iii) element *orientation*, if any; (iv) element *size*, estimated as the area of the region mask. Textures can be characterized by statistics computed on these features (averages or histograms, see in the following). It is worth specifying that different individual features and statistics could be adopted; in fact here we are not looking for “the best” set of features, but we are showing the portability and effectiveness of the general framework.

**Texel Grouping** The goal is to cluster texels with the same appearance, to capture choral spatial characteristics via layout attributes. Here we simply group texels according to the assigned class labels (*circle*, *line* or *polygon*). Only groups including at least 10 texels are kept, the other detections are removed.

**Layout description of texels.** To describe spatial patterns of each texel group, we measured attributes related to the spatial distribution of the texels’ centroids. Among the huge literature in statistics on spatial points patterns’ analysis to evaluate randomness, symmetry, regularity and more [2, 8, 28], we selected a simple yet general set of measurements. They are: (i) point *density*, *e.g.* the number of texels per area unit (for circles and polygons) or line density, *e.g.* the number of lines/bands along the direction perpendicular to their principal orientation (for lines). (ii) Quadratic counts-based *homogeneity* evaluation [14]: it amounts to divide the original image into 100 patches and perform a  $\chi^2$  test to evaluate the hypothesis of average point density in the sub-parts. Also in this case for lines, we estimated a similar 1D feature on the projection. (iii) Point pair statistics [14]: we estimate the point pair vectors for all the texel centers and then use them to estimate the histogram of *vectors orientation*. (iv) *Local symmetry*: for circles and polygons we considered the centroids’ grid and measured average reflective self-similarity of 4-points neighborhoods of points after their reflection around the central point. The distance function used is the average point distance, normalized by neighborhood size. Similarly, we measured *translational symmetry* by considering 4-point neighborhoods of the centroids and measuring the average minimum distance of their points from closest points in the grid after translations of the vectors defined by point pairs in the neighborhood. Symmetry descriptors are computed on 1D projections for line texels. The complete pattern descriptor is finally built joining texel attributes, spatial pattern attributes and the color attributes of the *background*. The dimensionality for each of these attributes is reported in Tab. 1. 1-dimensional attributes are averages of all the extracted values, while multi-dimensional ones are histograms. More details on these can be found as supplementary material. The Texel-Att descriptor is composed by concatenating the attributes and Z-normalizing each one of them.



Label Histogram	Color	Orientation Histogram	Size	Total	Density	Homogeneity	Vector Orientations	Local Symmetry	Traslational Symmetry	Background Color	Total
3	11	3	1	18	1	1	3	1	1	11	18

Table 1: Dimensionality of descriptor attributes. On the left, the attributes computed from the individual characterization of texels; on the right, attributes computed from statistics resulting from the spatial layout. The total dimensionality of the descriptor is 36.

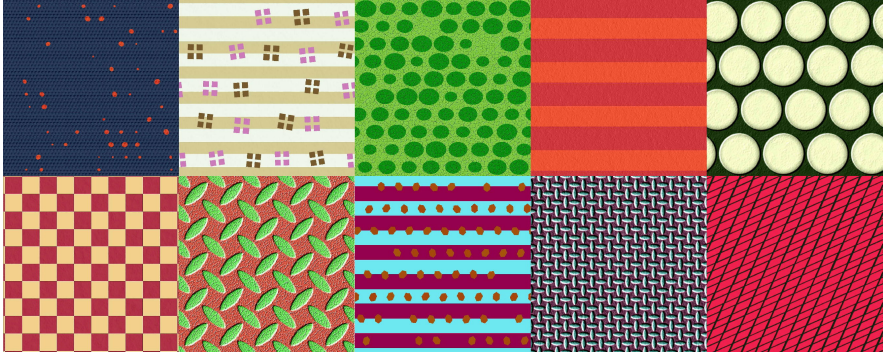


Figure 3: Images from the *ElBa* dataset.

### 3 Element-Based Texture Datasets: *ElBa* and E-DTD

While element-based textures are common and relevant to many practical applications (see Fig. 1), no public database focused on this texture domain is available. Existing databases as the DTD [5] include some examples of these textures (Fig. 1(a)), but these are mixed with other texture types. For these reasons, we build *ElBa*, the first dataset of element-based textures, and *E-DTD*, the element-based portion of the DTD dataset.

*ElBa* includes synthetic photo-realistic images, like those shown in Fig. 1(d). The advantages of dealing with synthetic textures are the precise annotations for texels by construction, and the possibility to train adequately a deep classifier, since training with synthetic data is a common practice [3, 26]. In particular, we propose a parametric synthesis model where we vary both texel *individual* (addressing the single texel) and *layout* attributes (describing how groups of texels are mutually displaced). As for individual attributes, we vary texel shape, size and orientation and color as follows. For the shape, inspired by the 2D shape ontology of [20], we consider general regular entities as *circles*, *lines*, *polygons* (squares, triangles, rectangles) since they can be thought of as approximations of more complicated shapes and because they encompass a large variety of geometric textiles. Size and orientation are varied linearly over a bounded domain. Colors are chosen from harmonized color palettes to better represent realistic use of colors. Texels are placed in 2D space based on a variety of layouts that can be described succinctly using symmetries. We consider both linear and grid-based layouts where the layout attributes are defined by one or two non-orthonormal vectors that define the translation between texels in the plane. This simple description represents several tiling of the plane and their corresponding patterns. We consider both regular and randomized distributions, where the randomization is performed by jittering the regular grid. By using jittering, we create a continuum between regular and non-regular distributions, and by varying the jitters per-texel we can change the stationarity.



Figure 4: Examples of E-DTD annotations: ground truth green bounding boxes overlaid to images of the classes *lined*, *dotted*, *honeycombed*, respectively.

Importantly, we take into account distributions of more than one element type arbitrarily combined in the plane. For example, we can create dotted+striped patterns. Each texel type has its own spatial layout attributes effectively creating arbitrary multi-class element textures (Fig. 1(d), Fig. 5-right).

We generate the images of *ElBa* using state-of-the-art computer graphics tools. We use Substance Designer for pattern generation<sup>2</sup>. Substance gives high-quality pattern synthesis, easy control and high-quality output including pattern antialiasing. High frequency patterns simulating realistic materials are added to the generated images.

This procedure led to a rough total of 30K of diverse textures rendered at a resolution of  $1024 \times 1024$ . The texture design process automatically provides ground-truth data for our analysis including texels masks, texels bounding boxes, and spatial distribution attributes. In total this amounts to around 3M annotated texels. It is very important to note that, differently from the other datasets used in the texture analysis domain, *ElBa* does not come with a rigid partition into classes: semantic labels that define relevant classification tasks like those used in our tests (Sec. 4.2) can be derived by texels’ attributes or by experiments with subjects.

The complete dataset is split in a training part (90%), used to train the network model and a test part (10%), used to validate the classification and recovery experiments.

To demonstrate our approach on real images, we created the Element-based DTD (E-DTD) as follows. From the DTD, we extracted textures that are element-based, i.e. characterized by a distribution or recognizable repeated texels with limited perspective distortions. We manually annotated the bounding boxes of each texel. E-DTD includes 1440 images belonging to 12 of the original DTD classes: *Banded*, *Chequered*, *Dotted*, *Grid*, *Honeycombed*, *Lined*, *Meshed*, *Perforated*, *Polka-dotted*, *Studded*, *Waffled*. These classes have been selected by 7 experts (3 graphic designers and 2 fashion experts and 2 computer scientists) with all of them agreeing on their inclusions. DTD classes with partial consensus have not been inserted into E-DTD. The annotation of texels was carried out by Mechanical Turk, borrowed from the three-phase ImageNet crowdsourcing annotation protocol [24]. The protocol consists of (1) a drawing phase, (2) a quality verification phase, where a second worker validates the goodness of the bounding boxes and (3) a coverage verification phase where a third worker verifies whether all object instances have bounding boxes. The annotation process produced around 900K texels annotations, some of which are shown in Fig. 4. It is important to note the very diverse types of bounding boxes, from very long and thin (addressing line texels)  $745 \times 5$  pixels bounding boxes to very small  $5 \times 5$  pixels bounding boxes (on tiny circles).

<sup>2</sup><https://www.allegorithmic.com/>

## 4 Experiments

Experiments focus on four aspects: 1) *detection of texels*, where we show that finding texels is nowadays possible, with a Mask-RCNN trained on *ElBa*; 2) *classification*, where we point out the failure of state-of-the-art descriptors in distinguishing textures which are clearly diverse against our Texel-Att that instead is succeeding; 3) *ranking*, where we demonstrate that Texel-Att representation ranks texture w.r.t. expressive yet fine-grained attributes; 4) *image search* where the Texel-Att attributes are exploited for accelerate human-in-the-loop image search [13] onto large image corpora.

### 4.1 Detection of texels

Detection performances have been computed on the testing partition of *ElBa* and on the whole E-DTD. The Mask-RCNN model used in these experiments has been trained on the training partition of *ElBa*. Fig. 5 reports some Texel-Att detection qualitative results, while Tab. 2 reports *per-image* average precision (AP): in practice, AP is computed *for each image*, and averaged over all the images, since we are interested in capturing how much *all of the texels of a single image* are detected, since it is crucial for computing the Texel-Att attributes afterwards. E-DTD dataset gives lower results, since it contains images with dramatic perspective deformation (see Fig. 5(a)), which was not a factor in the *ElBa* training data. Despite this, the next experiments show that such detection performance is enough to estimate attributes with high accuracy. Mask-RCNN trained on COCO gives dramatically low results (mAP = 1.75e-6), due to the completely different scenario, not reported in Tab. 2 for clarity. One may ask how Texel-Att detection works on a texture which is not element-based, like Fig. 1d. Few tests showed that the confidence of the detections, in that case, is definitely lower than in the element-based case, omitted here for the lack of space.

Dataset	mAP	AP50	AP75
E-DTD	0.53	0.63	0.40
<i>ElBa</i>	0.91	0.92	0.90

Table 2: Detection *per-image* average precision (see text) on E-DTD and *ElBa* datasets.

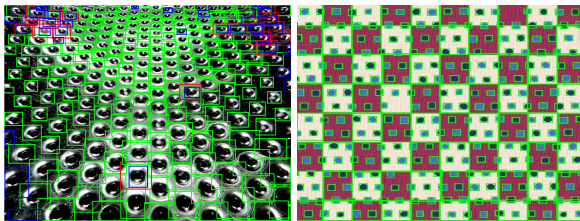


Figure 5: Texel-Att detection qualitative results on both E-DTD (left) and *ElBa* (right) datasets. In green the correct detections, in red the false positives (19 in the first, 0 in the second) and in blue the false negatives (35 in the first, 3 in the second). The AP(IoU=.50) are 0.81 and 0.99, respectively.

Classes	Tamura [12]	FV-CNN [4]	Texel-Att
Line uniformity	70.60	66.80	<b>85.30</b>
Circle positioning	54.86	53.01	<b>97.33</b>
Circle coloring	50.19	52.94	<b>93.42</b>

Table 3: Classification accuracy in three different binary tasks with three different approaches.

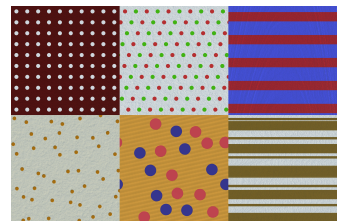


Figure 6: Images from the *ElBa* dataset, in columns: mono-colored regular and random circles, bi-colored regular and random circles, uniform and non-uniform lines.

## 4.2 Classification

On texel classification into *circles*, *polygons*, *lines* categories, Mask-RCNN scores a 99.85% of accuracy on almost 550K of correctly detected (IoU>0.5) texels. Class labels are used to organize texels into groups, as described in Sec. 2. Groups are described with layout attributes, and this completes the Texel-Att description. Three simple experiments on binary classification demonstrate the expressivity of Texel-Att, each one focusing on 200 *EIBa* images having strongly different attributes, that is *single-color VS bi-color circles*, *regularly VS randomly positioned circles* and *lines with uniform or non-uniform width* (see Fig. 6). Cross-validated 5-fold experiments compare the 36-dimensional Texel-Att description (see Tab. 1) against CNN+FV (65536-dimensional) and the Tamura [24] classic texture description. All of the three descriptors are fed into linear SVMs. Accuracies are shown in Tab. 3. Texel-Att obtains the best results as it captures higher visual semantics, i.e., the texels and how they are mutually related. FVs and Tamura features are not able to capture objects and spatial layout, focusing on filter outputs or directly on pixel values.

On E-DTD, Texel-Att description individuates strongly different textures within the same class, ideally defining further, finer-grained level of classes it can separate. For example the *dotted* and *banded* classes (see Fig. 1) are now further specified and classified considering big or small dots, regular or irregular bands. For lack of space, we prefer to skip the fine-grain classification experiments on the E-DTD (where we systematically beat the other descriptors) and instead present in the next section the more compelling experiments on ranking.

## 4.3 Ranking

Other than capturing fundamental properties of textures (for example, having regularly VS randomly placed texels, see the previous section), Texel-Att attribute values can be used to rank textures. Attributes that can be ranked are the basis for human-in-the-loop search strategies [24], so it is crucial that the ranking is reliable. Ideally, with the ground-truth texel detection the ranking via Texel-Att attributes will be perfect. In this experiment we evaluate how our detection step corrupts the ranking, and whether the ranking can be better estimated with learning based strategies, avoiding the detection step.

For simplicity, we consider here partial ranking; an attribute that induces partial ranking is said *relative* [24]; formally, given a set of images  $I=\{i, j\}$  and an *ideal* Texel-Att attribute  $a$  (i.e., computed on the ground-truth texel detection), there exists a partial order relation  $r_a^*$  such that  $i > j \iff r_a^*(i) > r_a^*(j) \wedge |r_a^*(i) - r_a^*(j)| > \gamma_a$ .

The goal of this experiment is to estimate a function  $r_a(i)$  as close as possible to  $r_a^*$ . Following the protocol of [24] the *ranking accuracy* of the function  $r_a$  is defined as the percentage of pairs correctly ordered by the  $r_a$  function over all the possible pairs in the set of images.

Two are the strategies we compare to estimate  $r_a$ : the first is the Texel-Att pipeline, which measures the attribute on top of the texel detections. The second is the relative attribute estimation of [24] using the FV-CNN [6] descriptor as input. For this second strategy we can assume  $x_i$  as the feature vector in  $\mathbb{R}^n$  for the image  $i$ . In this case  $r_a$  is *estimated* by a ranking SVM, following the guidelines in [24]. We assume  $r_a = w_a^T x_i$  so that the output of the modeling is the unknown vector  $w$ . The model is trained using the set of ordered pairs of images  $O_a = \{(i, j)\}$  where  $(i, j) \in O_a \Rightarrow i > j$  and the set of un-ordered pairs of images  $S_a = \{(i, j)\}$  where  $(i, j) \in S_a \Rightarrow i \sim j$ .

Attributes	Rank SVM [14]	Texel-Att	Attributes	Rank SVM [14]	Texel-Att
Area	65.52	<b>85.71</b>	Area	70.16	<b>93.86</b>
Local Symmetry	54.72	<b>64.29</b>	Local Symmetry	71.06	<b>81.71</b>
Homogeneity	79.91	<b>90.29</b>	Homogeneity	77.06	<b>96.86</b>
Mean	67.56	<b>81.68</b>	Mean	65.95	<b>84.55</b>

Table 4: Ranking accuracy of relative attributes on E-DTD (left) and *ElBa* (right) datasets.

We perform this experiment on the *ElBa* dataset (using the partitioning defined in Sec. 3) and the E-DTD dataset (randomly choosing 90% of the images as training set and the rest as testing set). We consider one attribute at a time. Ground truth  $r_a^*$  (i.e. ordered and unordered pairs) are computed from the ground truth detections also used in Section 4.1. The ranking accuracy across all attributes is shown in Tab. 4. It can be clearly seen that computing explicitly texel detection (i.e., following the Texel-Att pipeline) is the best strategy to rank textures according to the proposed attributes. For space reasons, only three attributes are shown on the table. The remaining ones are reported in the supplementary material.

#### 4.4 Texture Interactive Search

In this experiment we follow the Whittlesearch (WH) feedback scheme [14, 14] to search a texture among a large repository. It can be considered a coarse-to-fine user-initiated and iterative search, with each iteration at time  $t = 1, \dots, T$  presenting on a GUI the *target* image, simulating the user’s envisioned picture, and a *reference set*  $\mathcal{T}_t$  of  $n = 8$  images the user has to interact with by giving a feedback. At each iteration, top-ranked images are shown, until the target is ranked in the top  $n$  images, or the maximum iteration  $T = 10$  is completed. The WH scheme enriches traditional binary relevance feedback mechanism [14] by allowing the user to whittle away specific irrelevant portions of the visual feature space, pinpointing *how* different one image in  $\mathcal{T}_t$  is w.r.t. the target by using relative comparisons ("more", "equally", "less"), on a provided set of attributes. To prove that introducing Texel-Att attributes is beneficial to better describe textures, we set up a task of Interactive Image Search following the non-Active WhittleSearch variant [14], using our 36 attributes (see Table 1) estimated on top of the *detection* step. We compare with the attributes extracted from *ground-truth* annotations to understand how much a more accurate estimation leads to a better performance. We also compare with the 47 DTD attributes [5] employed here in their *relative* form (i.e., each attribute has a ranking function indicating how much it is expressed in the image) [14] and the 6 Tamura [14] attributes (*coarseness, contrast, directionality, linelikeness, regularity, roughness*). In particular we compare with three different variants: the 47 DTD attributes, the 6 Tamura attributes and the 47+6 DTD+Tamura attributes. The last combination is the most appealing, since the DTD attributes indicate the content of a texture (i.e., dots) and the Tamura attributes models low-level characteristics similar in spirit to ours (e.g., regularity) but computed on the pixels and not on texels. For all of these, each user is presented with a randomly chosen target image from the database. The goal is to navigate the database until the target image is found (i.e. it becomes one of the top  $n$  most relevant images in the database). A total of 50 unacquainted users participated in the study (mean age: 24, std: 1), after having performed a brief individual training session on the use of the interface. Each user had three trials and performances are averaged. Users were partitioned equally among the five approaches taken into consideration in this experiment. Following [14], performance



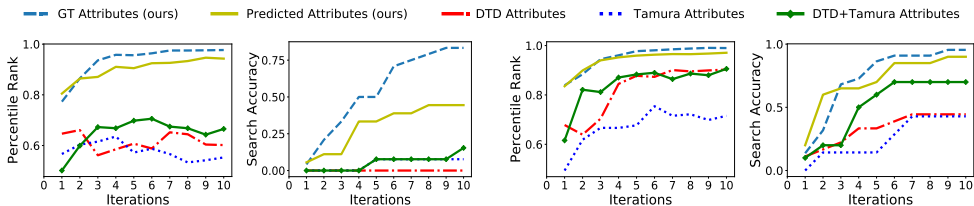


Figure 7: Texture Interactive Search (TIS) Percentile Rank and Search Accuracy results on *ElBa* (first two plots) and E-DTD (last two plots). On the x axis the number of feedback iterations. On the y axis the Percentile Rank index/Search accuracy score.

is measured using the percentile rank of the target image (i.e. the fraction of the database images ranked below the target) after a fixed number of interaction steps. The closer to 100%, the better the result. We also compute Search Accuracy: by considering 40 images as the size of a typical image search page [14], a texture is considered as "found" by the search if it is ranked among the first 40 images. Keeping this in mind we find that on the E-DTD dataset we are able to individuate within 10 iterations the desired texture in the 90% of cases while using the most performing variant's (DTD+Tamura) attributes accuracy drops down to 71%. On the *ElBa* dataset, which is much more challenging on this task due to the larger size of the pool of images and the finer grained nature of the textures, we are able to reach 44% accuracy, while the DTD+Tamura attributes reach only 15%. The plot in Fig. 7 shows that Texel-Att has the best performance at any iteration. In addition, a good performance is preserved even in the case of predicted attributes, confirming the robustness of the approach against imperfect texel detection. Finally, on average we are able to individuate the desired texture more often with our approach than with other techniques.

## 5 Discussion

This paper presents a new way to describe textures, adopting attributes which focus on texels. The proposed framework, Texel-Att, can successfully describe and classify patterns that are not well-handled by the existing texture analysis approach, as demonstrated by the experimental results, supported also by two new datasets, *ElBa* and E-DTD. In addition, Texel-Att is showed to be highly effective for image search, paving the way to fashion and graphic design applications. The current implementation has much room for improvement, being trained with few texel types (circles, lines, polygons) and 2D patterns with limited distortions. In fact, the modular design of the framework makes it easy to customize it for handling different kinds of element-based texture, as it is just a matter of changing the detector to localize and group different texel types, and changing the invariance properties of the layout attributes to handle larger distortions.

**Acknowledgements:** This work has been partially supported by the project of the Italian Ministry of Education, Universities and Research (MIUR) "Dipartimenti di Eccellenza 2018-2022", and has been partially supported by the POR FESR 2014-2020 Work Program (Action 1.1.4, project No.10066183). We also thank Nicolò Lanza for assistance with Substance Designer software.



## References

- [1] Narendra Ahuja and Sinisa Todorovic. Extracting texels in 2.1 d natural textures. In *2007 IEEE 11th International Conference on Computer Vision*, pages 1–8. IEEE, 2007.
- [2] Adrian Baddeley, Ege Rubak, and Rolf Turner. *Spatial point patterns: methodology and applications with R*. Chapman and Hall/CRC, 2015.
- [3] Igor Barros Barbosa, Marco Cristani, Barbara Caputo, Aleksander Rognhaugen, and Theoharis Theoharis. Looking beyond appearances: Synthetic training data for deep cnns in re-identification. *Computer Vision and Image Understanding*, 167:50–62, 2018.
- [4] Richard Bormann, Dominik Esslinger, Daniel Hundsdoerfer, Martin Haegele, and Markus Vincze. Robotics domain attributes database (rdad), 2016. [http://wiki.ros.org/ipa\\_texture\\_classification](http://wiki.ros.org/ipa_texture_classification).
- [5] Mircea Cimpoi, Subhansu Maji, Iasonas Kokkinos, Sammy Mohamed, and Andrea Vedaldi. Describing textures in the wild. In *Proceedings of the IEEE Conference on Computer Vision and Pattern Recognition*, pages 3606–3613, 2014.
- [6] Mircea Cimpoi, Subhansu Maji, and Andrea Vedaldi. Deep filter banks for texture recognition and segmentation. In *The IEEE Conference on Computer Vision and Pattern Recognition (CVPR)*, June 2015.
- [7] Mircea Cimpoi, Subhansu Maji, Iasonas Kokkinos, and Andrea Vedaldi. Deep filter banks for texture recognition, description, and segmentation. *International Journal of Computer Vision*, 118(1):65–94, 2016.
- [8] Peter J Diggle et al. *Statistical analysis of spatial point patterns*. Academic press, 1983.
- [9] Yan Gui, Mingang Chen, Lizhuang Ma, and Zhihua Chen. Texel based regular and near-regular texture characterization. In *2011 International Conference on Multimedia and Signal Processing*, volume 1, pages 266–270. IEEE, 2011.
- [10] Kaiming He, Georgia Gkioxari, Piotr Dollár, and Ross Girshick. Mask r-cnn. In *Computer Vision (ICCV), 2017 IEEE International Conference on*, pages 2980–2988. IEEE, 2017.
- [11] Takashi Ijiri, Radomír Mech, Takeo Igarashi, and Gavin Miller. An example-based procedural system for element arrangement. In *Computer Graphics Forum*, volume 27, pages 429–436. Wiley Online Library, 2008.
- [12] Janine Illian, Antti Penttinen, Helga Stoyan, and Dietrich Stoyan. *Statistical analysis and modelling of spatial point patterns*, volume 70. John Wiley & Sons, 2008.
- [13] Adriana Kovashka, Devi Parikh, and Kristen Grauman. Whittlesearch: Image search with relative attribute feedback. In *2012 IEEE Conference on Computer Vision and Pattern Recognition*, pages 2973–2980. IEEE, 2012.
- [14] Adriana Kovashka, Devi Parikh, and Kristen Grauman. Whittlesearch: Interactive image search with relative attribute feedback. *International Journal of Computer Vision*, 115(2):185–210, 2015.

- [15] Li Liu, Jie Chen, Paul W. Fieguth, Guoying Zhao, Rama Chellappa, and Matti Pietikäinen. A survey of recent advances in texture representation. *CoRR*, abs/1801.10324, 2018. URL <http://arxiv.org/abs/1801.10324>.
- [16] Siying Liu, Tian-Tsong Ng, Kalyan Sunkavalli, Minh N Do, Eli Shechtman, and Nathan Carr. Patchmatch-based automatic lattice detection for near-regular textures. In *Proceedings of the IEEE International Conference on Computer Vision*, pages 181–189, 2015.
- [17] Hugo Loi, Thomas Hurtut, Romain Vergne, and Joelle Thollot. Programmable 2d arrangements for element texture design. *ACM Trans. Graph.*, 36(4), May 2017. ISSN 0730-0301. doi: 10.1145/3072959.2983617. URL <http://doi.acm.org/10.1145/3072959.2983617>.
- [18] Chongyang Ma, Li-Yi Wei, and Xin Tong. Discrete element textures. *ACM Trans. Graph.*, 30(4):62:1–62:10, July 2011. ISSN 0730-0301. doi: 10.1145/2010324.1964957. URL <http://doi.acm.org/10.1145/2010324.1964957>.
- [19] Chongyang Ma, Li-Yi Wei, Sylvain Lefebvre, and Xin Tong. Dynamic element textures. *ACM Trans. Graph.*, 32(4):90:1–90:10, July 2013. ISSN 0730-0301. doi: 10.1145/2461912.2461921. URL <http://doi.acm.org/10.1145/2461912.2461921>.
- [20] Tim Matthews, Mark S Nixon, and Mahesan Niranjan. Enriching texture analysis with semantic data. In *Proceedings of the IEEE Conference on Computer Vision and Pattern Recognition*, pages 1248–1255, 2013.
- [21] M. Niknam and C. Kemke. Modeling shapes and graphics concepts in an ontology. In *SHAPES*, 2011.
- [22] Devi Parikh and Kristen Grauman. Relative attributes. In *Computer Vision (ICCV), 2011 IEEE International Conference on*, pages 503–510. IEEE, 2011.
- [23] Arnold WM Smeulders, Marcel Worring, Simone Santini, Amarnath Gupta, and Ramesh Jain. Content-based image retrieval at the end of the early years. *IEEE Transactions on Pattern Analysis & Machine Intelligence*, (12):1349–1380, 2000.
- [24] Hao Su, Jia Deng, and Li Fei-Fei. Crowdsourcing annotations for visual object detection. In *Workshops at the Twenty-Sixth AAAI Conference on Artificial Intelligence*, 2012.
- [25] Hideyuki Tamura, Shunji Mori, and Takashi Yamawaki. Textural features corresponding to visual perception. *IEEE Transactions on Systems, man, and cybernetics*, 8(6): 460–473, 1978.
- [26] Jonathan Tremblay, Aayush Prakash, David Acuna, Mark Brophy, Varun Jampani, Cem Anil, Thang To, Eric Cameracci, Shaad Boochoon, and Stan Birchfield. Training deep networks with synthetic data: Bridging the reality gap by domain randomization. In *Proceedings of the IEEE Conference on Computer Vision and Pattern Recognition Workshops*, pages 969–977, 2018.

- 
- [27] Joost Van De Weijer, Cordelia Schmid, Jakob Verbeek, and Diane Larlus. Learning color names for real-world applications. *IEEE Transactions on Image Processing*, 18(7):1512–1523, 2009.
- [28] Eduardo Velázquez, Isabel Martínez, Stephan Getzin, Kirk A Moloney, and Thorsten Wiegand. An evaluation of the state of spatial point pattern analysis in ecology. *Ecography*, 39(11):1042–1055, 2016.
- [29] Peng Zhao and Long Quan. Translation symmetry detection in a fronto-parallel view. In *CVPR 2011*, pages 1009–1016. IEEE, 2011.